Proc. Natl. Acad. Sci. USA
Vol. 92, pp. 6887–6891, July 1995
Biophysics

Trapping of branched DNA in microfabricated structures

(electrophoresis/electrostatic trapping/DNA topology)

W. D. VOLKMUTH†, T. DUKE†‡§, R. H. AUSTIN†, AND E. C. COX‡§

Departments of †Physics and ‡Molecular Biology and §Program in Materials Science, Princeton University, Princeton, NJ 08544-0708

Communicated by Hans Frauenfelder, Los Alamos National Laboratory, Los Alamos, NM, January 17, 1995 (received for review June 27, 1994)

ABSTRACT **We have observed electrostatic trapping of tribranched DNA molecules undergoing electrophoresis in a microfabricated pseudo-two-dimensional array of posts. Trapping occurs in a unique transport regime in which the electrophoretic mobility is extremely sensitive to polymer topology. The arrest of branched polymers is explained by considering their center-of-mass motion; in certain conformations, owing to the constraints imposed by the obstacles a molecule cannot advance without the center of mass first moving a short distance backwards. The depth of the resulting local potential well can be much greater than the thermal energy so that escape of an immobilized molecule can be extremely slow. We summarize the expected behavior of the mobility as a function of field strength and topology and point out that the microfabricated arrays are highly suitable for detecting an extremely small number of branched molecules in a very large population of linear molecules.**

Accurate fractionation of DNA molecules is vital to research in molecular biology. DNA with length ranging from a single base to many millions of bases can be separated by electrophoresis, for both preparative and analytical purposes. Successful fractionation requires a medium that restricts the motion of the molecules as they migrate under the influence of the electric field. Traditionally, a gel has been used, and the numerous variants of gel electrophoresis have become some of the most widely used techniques in molecular biology. Recently, we introduced the technology of microfabricated restrictive environments (1) to facilitate the study of the electrophoresis of long polymers. Microlithographic etching of silicon wafers enables the creation of a precisely controlled "obstacle course" which can be used as a substitute for the gel. The two-dimensional structure allows the clear visualization of the molecular dynamics by fluorescence microscopy. Our primary aim is to develop devices which will permit rapid separation of chromosomal DNA molecules according to size, a task which cannot readily be accomplished by using a gel. In this paper, we demonstrate that such arrays can be used to examine the fractionation of DNA according to topology. By contrasting the dynamics of linear and branched DNA, we present striking evidence that long polymers in a regular array of posts have a mobility that depends on their topology.

Previously, experimental data in gels have demonstrated that the electrophoretic mobility is independent of topology if the polymers are weakly entangled with the network (2)—i.e., if their radius of gyration R is comparable with the mesh size a. Unentangled molecules ($R < a$) have a topology-dependent mobility (3), as do strongly entangled polymers ($R > a$) (4, 5). The latter result can be understood in terms of the reptation model, which describes the diffusion of polymers in a constrictive environment: linear molecules (6), rings (7), and stars (8) each diffuse by a different reptative mechanism. The topology dependence that we observe in our microstructures occurs in a quite different transport regime. This is a consequence of the openness of the structures and the long length of the DNA molecules we used. Obstacles hem in the polymers only if the field is weak. The field may be characterized by the dimensionless parameter $\varepsilon = \lambda E a^3/PkT$ (9, 10) and a "weak" field refers to the case $\varepsilon \ll 1$. Here, $\lambda \approx 0.3\ e^-/Å$ (11) is the charge per unit length, $P \approx 60$ nm (12, 13) is the persistence length, a is the average pore spacing and kT is the thermal energy [a more complete discussion of these parameters and their magnitude can be found in a previous publication (14)].

For the scale of obstacles we used ($a \sim 1\ \mu m$), $\varepsilon \gg 1$ even at moderate values of the applied field. In this case the reptation picture no longer applies, since loops of the polymer can readily slip between obstacles. The dominant mode of transport in this regime involves the hooking of molecules around a post (14, 15). When a long linear DNA molecule with contour length L gets hooked, it unwinds to form a U-shaped configuration. A tension develops in each arm, increasing from zero at the dangling ends to a value of order λEL at the point where the chain passes over the post. The parameter $\kappa = kT/\lambda EP$ characterizes the length scale above which the tension overcomes the Brownian forces and stretches the chain. κ can be surprisingly small, about 1 μm for very modest fields on the order of 1 V/cm. Note that since the rise per base pair in B-form DNA is roughly 3.4 Å per base pair, this means that only the 3000 bp adjacent to each end of the molecule are randomly coiled. Long molecules with $L \gg \kappa$ get almost completely stretched when they hook. We demonstrate that in this transport regime, the hooking dynamics of a branched polymer can lead it into a situation in which it is electrostatically trapped. Whichever way the polymer attempts to move, its center of mass backs up against the field so that its potential energy increases. Trapping can last for very long times since the depth of the potential well can be much greater than the thermal energy. Moreover, the electrophoretic mobility of a branched polymer is even more strongly quenched in this case than in the reptation regime, decreasing exponentially with the square of the length of the shortest branch.

Sample Preparation and Measurements

The DNA samples were prepared by incubating bacteriophage λ DNA at a concentration of 5 μg/ml in 1× T4 ligation buffer (containing 1 mM ATP) with 10 units of T4 DNA ligase per ml (ligase, buffer, and DNA were all purchased from New England Biolabs). The samples were ligated at 16°C for approximately 12 h, stained with ethidium bromide, and imaged by epifluorescence microscopy in an array of posts, as described in ref. 1.

A very small fraction of the ligated molecules were branched. A total of 12 were observed mixed in among many thousands of linear polymers. Of the branched molecules, most had three segments connected at a single point so that they were Y shaped. The complex kinetics associated with the formation of the junction explains the rarity of branched molecules (Fig. 1).

The publication costs of this article were defrayed in part by page charge payment. This article must therefore be hereby marked "*advertisement*" in accordance with 18 U.S.C. §1734 solely to indicate this fact.

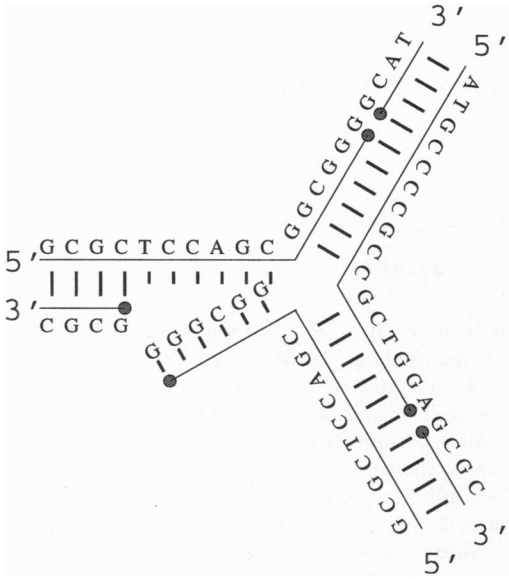

FIG. 1. Possible structure of the three-arm junction. Bacteriophage λ has sticky ends that are 12 bases long. We believe that the sticky ends allow two molecules to be ligated onto the end of a third. Circles indicate the nicks that are joined by the ligase. In the above, three base pair mismatches would occur if a completely closed structure were formed, although two of the three mismatches would still be purine·pyrimidine pairs.

The array of posts was etched from silicon by using standard microfabrication techniques. The posts were 1.0 μm in diameter, had 2.0-μm center-to-center spacing, and were 0.150 μm in height. Arrays of sizes from 1 cm × 2 cm to 2 cm × 6.5 cm were fabricated and mounted in a holder having a buffer well at either end, with electrodes in the wells. The DNA was confined to migrate among the posts by a Pyrex coverslip covalently bonded to the tops of the posts. DNA was loaded into the microfabricated chamber by placing a 2-μl volume of DNA in electrophoresis buffer at the edge of the Pyrex coverslip and allowing the sample to wick into the chamber.

Electrical contact to the microfabricated electrophoretic chamber was made by bridging each buffer well with a second coverslip butted up against the Pyrex coverslip. Surface tension held the buffer against the coverslip, giving low-resistance contact to the array so that most of the voltage applied to the electrodes was dropped over the array.

Condition for Trapping to Occur

Fig. 2 shows epifluorescence micrographs of branched molecules. The three segments of a molecule are stretched out in the electric field and the molecule itself looks like two hooked Us joined together. Some of the molecules in the figure were trapped. Molecule *a*, for example, showed no center-of-mass motion over a 30-min period in an applied field of about 1 V/cm. By comparison, a linear molecule in this field has a free-draining velocity $V_{max} \approx 5$ μm/s and travels through the array of posts at a somewhat lower speed, around 3 μm/s, as a result of temporarily slowing up when hooked on posts (14). After observing no motion of molecule *a* for 30 min, we reversed the field. The molecule moved backwards a short distance, about 5 μm, but quickly became trapped again.

Trapping of branched molecules can be explained by considering how a molecule must move to extricate itself from a hooked conformation. A trapped molecule is drawn schematically in Fig. 3. We number the segments as follows: 1, the segment forming the top U hook; 2, the longer segment of the lower U hook; and 3, the shorter segment. Denoting the contour lengths of the segments l_1, l_2, and l_3, the total length

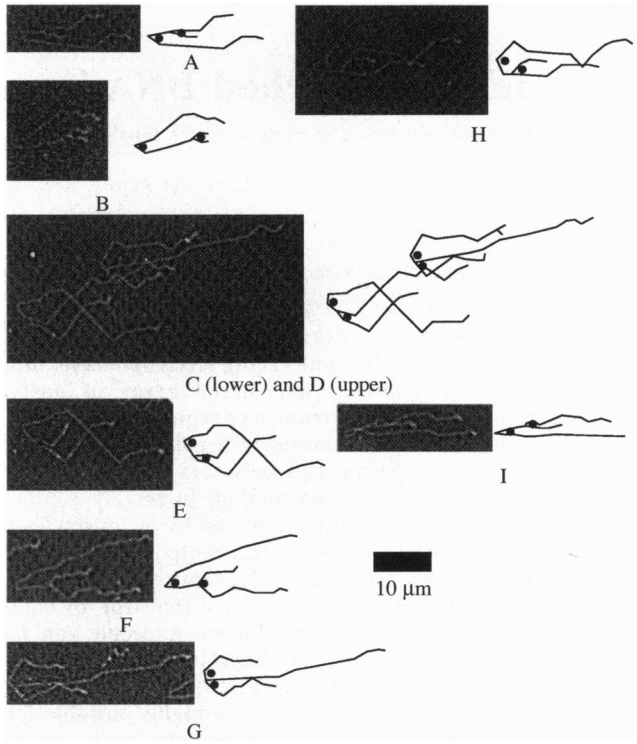

FIG. 2. Trapped molecules. The array of posts is faintly visible in negative relief due to background dye in the DNA-containing buffer solution. The center–center post spacing is 2 μm. The pictures have been processed by a sharpening filter. Adjacent to each micrograph is a sketch of the corresponding branched molecule(s). The dots in the sketch indicate the posts on which the molecules are hung. Scale bar is 10 μm.

of the molecule is $L = l_1 + l_2 + l_3$. We label the free ends E_1, E_2, E_3 and the junction J. The z axis is chosen along the field direction with increasing z in the direction of motion of the molecule. Let $x = z(E_1) - z(E_2)$ be the distance between E_2 and E_1 along the z axis, and x_0 be the initial value of x immediately after the branched molecule hooks.

We assume that the arms of the molecule all hang straight down; later we shall comment on how this approximation affects the analysis. The three ways in which unhooking can occur are drawn in Fig. 3. Configuration A can advance by sliding toward E_1 (process A → A_1), toward E_2 (process A → A_2), or toward E_3 (process A → A_3). A branched DNA molecule will be trapped if motion along all of these paths is energetically unfavorable.

Consider the first two possibilities. The important feature to remark is that whether the molecule slides toward E_1 or toward E_2, the topology obliges segment 3 to move backwards against the field. Since the sliding of segment 3 transfers DNA from $z(E_3)$ to $z(J)$, it increases the potential energy by an amount proportional to l_3. Sliding of the rest of the chain towards E_1, on the other hand, transfers DNA from $z(E_2)$ to $z(E_1)$ and decreases the potential energy by an amount proportional to x_0. Thus, the overall change in potential energy is negative along the path A → A_1 only if $x_0 > l_3$. Similarly, sliding towards E_2 decreases the potential energy by an amount proportional to $-x_0$ and A → A_2 will be energetically favorable only if $-x_0 > l_3$. Combining these two conditions, we find that the DNA will not move along either path if

$$|x_0| < l_3. \quad [1]$$

Consider now the final possibility A → A_3. We note that this is distinguished from A → A_2 by the fact that the lower U (formed by segments 2 and 3) moves in the opposite direction.

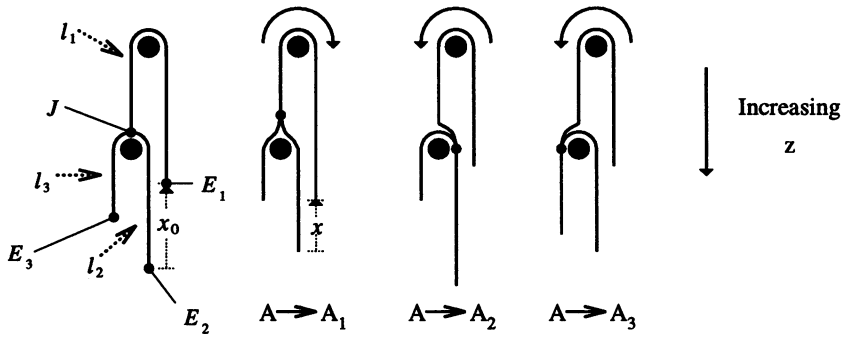

FIG. 3. The three processes by which a branched molecule can unhook. The labels l_1, l_2, and l_3 refer to the contour lengths of the segments, and the total length $L = l_1 + l_2 + l_3$. x is the distance between the ends of l_1 and l_2 along the direction of motion, and x_0 is the initial value of x. As discussed in the text, when $l_3 > |x_0|$ the molecule will be trapped because z_{cm} must decrease.

From our definition of the segment lengths, sliding of the lower hook towards E_3 is always less favorable than sliding towards E_2. Thus A → A$_3$ cannot provide an alternative path for spontaneous motion when relation **1** is satisfied. Relation **1** is therefore the universal trapping condition.

Trapping Lifetime

When the trapping condition is satisfied, a molecule must overcome an electrostatic potential barrier to move along any of the three paths. As calculated by Kramers (16), the time τ for a particle to escape a potential well with a single barrier height $\Delta U \gg kT$ is

$$\tau = \tau_0 e^{\Delta U/kT}, \qquad [2]$$

where τ_0 is a characteristic time scale, which we shall determine below.

Using Eq. **2**, we can estimate the time required for a branched molecule to escape. Our aim is to demonstrate that the trapping lifetimes of the observed molecules can be extremely long. Roughly, the total escape rate is the sum of the escape rates over each of the individual barriers as calculated by using Eq. **2**. Since the rates depend exponentially on barrier height, the rate over the lowest barrier height will dominate the overall rate when all of the barriers are much larger than kT. The rate of escape due to process A → A$_3$ is negligible except when $l_2 - l_3 < \kappa$, so it is ignored in what follows.

Since the field is uniform and the DNA is uniformly charged, the electrostatic potential energy U depends only on the location of the center of mass z_{cm}:

$$U = \lambda E L z_{cm}. \qquad [3]$$

Thus, the depth and form of the potential well can be determined by considering the motion of the center of mass of the DNA as it extricates itself from the trap.

Along A → A$_1$, a small change in x, of magnitude dx, effectively results in the transposition of amount dx/2 of chain from $z(E_2)$ to $z(E_1)$ and the same amount from $z(E_3)$ to $z(J)$. Thus,

$$\frac{dz_{cm}^{A\to A_1}}{dx} = \frac{1}{2L}(x - l_3). \qquad [4]$$

Along path A → A$_2$, segment 3 is pulled over the post into a U shape, so that when one considers the transfer of mass from $z(E_1)$ to $z(E_2)$ and from $z(E_3)$ to $z(J)$, one finds

$$\frac{dz_{cm}^{A\to A_2}}{dx} = \frac{1}{2L}(2x - x_0 + l_3). \qquad [5]$$

Integration of Eqs. **4** and **5** with respect to x gives Δz_{cm} and hence ΔU from Eq. **3**

$$\frac{\Delta U(x)}{kT} = \begin{cases} \dfrac{\lambda E}{4kT}[-(x - l_3)^2 + (x_0 - l_3)^2] & x_0 < x < l_3 \\ \dfrac{\lambda E}{8kT}[-(2x - x_0 + l_3)^2 + (x_0 + l_3)^2] & -l_3 < x < x_0. \end{cases} \qquad [6]$$

The potential well is plotted in Fig. 4 for values of l_3 and x_0 taken from the entry for molecule i in Table 1 summarizing the measurement results.

The barrier height ΔU for each process is given by $U(x^*) - U(x_0)$, where x^* is the point at which dz_{cm}/dx = 0:

$$\frac{\Delta U^{A\to A_1}}{kT} = \frac{\lambda E}{4kT}(x_0 - l_3)^2 \qquad [7]$$

$$\frac{\Delta U^{A\to A_2}}{kT} = \frac{\lambda E}{8kT}(x_0 + l_3)^2. \qquad [8]$$

An approximate escape time for trapped DNA is given by Eq. **2** where ΔU is the smaller of the two barriers in Eqs. **7** and **8**:

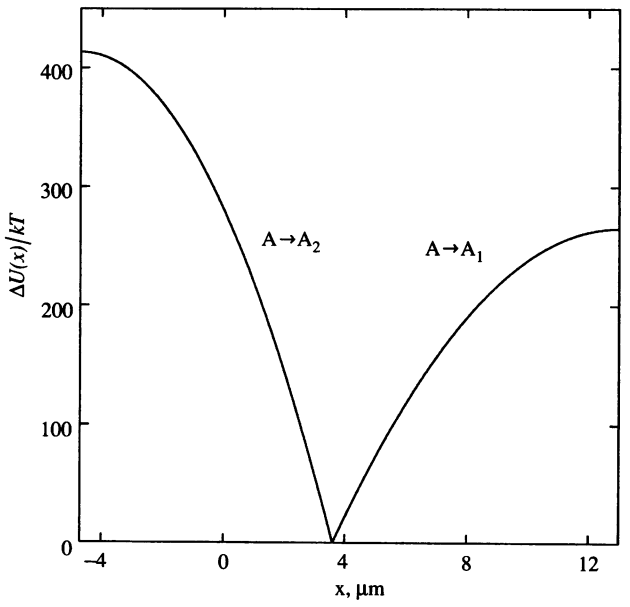

FIG. 4. The potential energy $U(x)/kT$ along the two most likely paths to unhooking for molecule i in Table 1.

Table 1. Summary of measurements for observed branched DNA molecules

Molecule	l_3, μm*	x_0, μm†	$\Delta U_{min}/kT$
a	8.9	7.1	9.7 ± 3.7
b	5.8	3.0	23.5 ± 5.8
c	33.2	−3.7	1300 ± 30
d‡	27.7	−28.1	NA§
e	15.1	13.2	1.9 ± 1.7
f	14.1	6.9	155 ± 15
g	26.4	−37.5	NA§
h	13.6	13.0	1.1 ± 1.2
i	13.0	3.6	265 ± 20

*Measurements for l_3 are ±0.2 μm.
†Measurements for x_0 are ±0.3 μm.
‡See note in text regarding molecule *d*, which is not actually a Y-shaped molecule.
§NA, not applicable.

$$\Delta U = Min\{\Delta U^{A\rightarrow A_1}, \Delta U^{A\rightarrow A_2}\}. \quad [9]$$

The value of τ_0 may be estimated as $\tau_0 = d^2/2D$, where D is the curvilinear diffusion coefficient of the polymer as it slithers around the obstacles and d is the typical distance that the molecule can slide under the influence of thermal forces. Previous results have demonstrated that DNA is free draining in the array of posts (14), so that $D = kT/3\pi\eta L$. From Eq. **7**, we obtain $d^2 \approx 4kT/\lambda E$. Thus $\tau_0 \approx 6\pi\eta L/\lambda E$. A more precise value of the prefactor may be obtained by using the Smoluchowski equation, which governs diffusion in a potential, to calculate the mean first passage time out of the well (16). This detailed analysis shows that Eq. **2** can be expressed as

$$\tau \approx \frac{12\pi\eta L}{\lambda E}\left(\frac{\pi kT}{2\Delta U}\right)^{1/2} e^{\Delta U/kT}, \quad (\Delta U/kT \gg 1). \quad [10]$$

We know that the limiting velocity of DNA in an array of posts is given by the free-draining result $V_{max} = \lambda E/3\pi\eta$ ($\eta = 1.0 \times 10^{-2}$ poise for aqueous solution), so from the observed value $V_{max} \approx 5.0$ μm/s in a field $E \sim 1$ V/cm, we estimate $\tau_0/L \approx 1.0(\Delta U/kT)^{-1/2}$ s/μm.

Experimental Results

The segment lengths that we measured for the Y-shaped molecules were different from the expected multiples of monomeric λ length of 16 μm. The discrepancy is probably due to shearing during pipetting. Also, we occasionally observed photolytic cleavage. Some molecules with four segments were observed. One of these, molecule *d* in Fig. 2, had two separate junctions and was H shaped. The center segment of the H measured 33.0 ± 0.3 μm, as expected if our hypothesis about junction formation is correct, since the molecule would consist of two Y junctions with a λ dimer linking them. Some X-shaped, four-branched molecules were observed in which the arms appeared to come together in a junction at a single point. Possibly, the fourth segment was ligated on to the dangling end left over from junction formation involving three strands.

The trapping time τ given by Eq. **10** is very much longer than experimental run times when the barrier height is much greater than kT. Table 1 gives a summary of the measured parameters and calculated barrier heights for several molecules. Fig. 5 plots pairs of l_3 and x_0 values from Table 1. Strictly speaking, all molecules are only metastable. The points labeled "unstable" correspond to molecules that were observed to have noticeable center-of-mass motion during observation. Two of the three unstable molecules lie just above the line $l_3 = |x_0|$, but they have barrier heights that are comparable to kT. Molecule *d* lies in the unstable region for tribranched molecules but was observed to be stable. As mentioned above, this

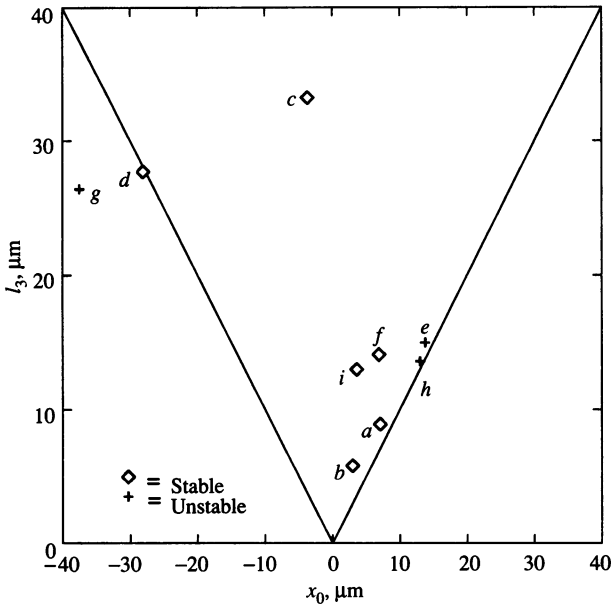

FIG. 5. Scatter plot of l_3, x_0 pairs from Table 1. The solid line is a plot of $l_3 = |x_0|$. Above the line a potential barrier exists, below the line there is no barrier.

molecule had a short fourth branch ligated onto the end of segment 1, which could be seen on the images recorded on videotape but is only faintly visible in the figure (note the brightened end). The length of the short branch is 3–4 μm, just enough to change the center of mass so that the molecule traps. After about 20 min, l_1 on molecule *d* broke, resulting in molecule *g*, observed to be unstable as expected for a molecule with $l_3 \ll |x_0|$ and it escaped in about 20 s. Similarly, molecule *e* resulted from l_2 breaking in molecule *c*. Molecule *e* had a small barrier height and was observed to unhook after about 30 s along path $A \rightarrow A_1$. The mean escape time predicted from Eq. **10** is $\tau = 500$ s. There is not an unreasonable difference between our results and the predicted behavior, given that Eq. **10** should only hold for $\Delta U/kT \gg 1$.

Although our analysis contains some simplifications, it demonstrates the essential physics of trapping and correctly predicts the condition under which a polymer will be immobilized. Specifically, a three-branched molecule becomes trapped when $|x_0| < l_3$, because sliding towards any one of the three ends requires the center of mass to reverse against the force field. The highest barrier encountered by a tribranched molecule as it moves through the array scales as the square of its shortest arm length l_3, so that for a DNA molecule in a field of about 1 V/cm, this barrier considerably exceeds thermal energies when l_3 is larger than a few micrometers. It should be added that polymers with more than three segments should get trapped for the same reasons that a tribranched polymer does, as we in fact observed for a four-branched polymer.

The most significant approximation in determining the barrier height comes from assuming that the arms of the molecules hang straight down. As seen in Fig. 2, this is never exactly the case, and in fact the arms often have several bends. ΔU is thus overestimated since Δz_{cm} is actually less than calculated above, and consequently the escape time τ is shorter.

Discussion

In general, motion of long-branched polymers in a gel can be characterized by the dimensionless field strength ε and the values l_i/κ, which measure the degree of stretching of the arm segments with the field (17). In the limit of zero field, the mobility is related to the equilibrium diffusion coefficient by

the Nernst–Einstein relation. For a linear polymer, the reptation theory of de Gennes (6) predicts $\mu \sim 1/L$ (18), and low-field mobility measurements give good agreement with this prediction (19). However, for a branched polymer with one side chain of length l_3, reptation theory predicts that $\mu \sim e^{(-l_3 P/a^2)}$, so that the low-field mobility is greatly reduced by the side chain (8). The reason is that entropically, it is more favorable for the shortest branch to inhabit a separate tube from the other two arms. Then the polymer can undergo translational motion only during the rare moments that the side branch retracts completely down its tube to the junction point. At intermediate field strengths, such that $\varepsilon \ll 1$ but $l_i/\kappa > 1$, sufficient tension can develop at the junction to counteract the entropic force and pull the shortest arm into the same tube as the others, so that the polymer reptates as a linear chain. In this case the mobility depends inversely on the polymer length for short molecules and becomes independent of length for longer molecules (20, 21). It is only when $\varepsilon > 1$ and $l_i/\kappa \gg 1$ for each i that the analysis presented in this paper should hold, since then the field is strong enough to pull loops of the molecule out of the tube so that the double hooks can form and the arms will be highly oriented along the field. So overall, one expects that the mobility as a function of ε for a given length l_3 starts out exponentially small, then increases to the linear polymer regime, and finally decreases exponentially to zero once trapping begins to occur.

Our observation of the trapping of large branched DNA molecules may shed some light on the mechanism of arrest of megabase-size DNA in agarose gels. It is known that extremely long linear DNA chains will migrate through a gel only if the field is very weak; otherwise, they get trapped. Furthermore, it has been demonstrated that the arrest can be irreversible: once halted, a molecule cannot be displaced again regardless of how the field is manipulated (22). The refusal of long DNA to migrate at moderate field strengths poses a severe problem and effectively restricts the gel electrophoresis technique to molecules shorter than ≈10 Mb. It has previously been suggested that the formation of knots may be responsible for this failing (22), and our observations suggest an explanation of how knotting can lead to arrest. It has been established that during agarose gel electrophoresis (and especially pulsed-field electrophoresis) a long DNA molecule typically advances through the gel at many locations simultaneously by the protrusion of loops or "hernias" (23). The tips of the hernias search for a pathway through the gel just like the free ends of the chain. Just as it is easy to tie a knot near a free end, so it is likely that random thermal motion creates a knot near a hernia tip. Usually, Brownian motion ensures that such a knot remains loose (a "slip knot," as it were) so that the DNA conformation can continue to evolve unimpeded. Thus, the hernia continues to grow as more chain slips through the knot. The action of the field on the resulting highly extended conformation produces a chain tension that may be sufficiently elevated to "tighten" the knot. By this, we mean that the high tension may induce an irreversible conformational change on the scale of the DNA thickness d, as suggested by Viovy *et al.* (22) (one would expect this to occur when $\lambda LEd \gg kT$). If the knot tightens and ceases to slip, the DNA resembles a tribranched molecule, although it differs in that one of the arms is actually a doubled-up loop. Thus, one would expect it to get trapped in the gel by the mechanism described in this paper, with a trivial alteration of the trapping condition relating to the doubled charge density in one of the arms. The interesting point about this explanation of the arrest of megabase-size molecules in gel electrophoresis is that it demands no specific interaction between the DNA and the gel, nor even a topological interaction as the DNA need not get tied around a gel fiber. The self-interaction of the DNA under conditions of high tension, induced by the interplay of the driving field and the restraining gel fibers, is sufficient to cause an effective change of DNA topology, which in turn leads to electrostatic trapping.

Finally, we point out that immobilized molecules are easily seen in our arrays, since all other molecules move steadily in the direction of the applied force. The methodology used here is thus a very sensitive way to detect exceedingly small numbers of branched molecules mixed in with a large number of linear molecules. It could in principle be used both as an analytical device and a preparative tool to examine and purify three-branched molecules that are known to arise during denaturing gradient gel electrophoresis (24, 25), DNA replication, recombination, and repair.

We thank Blake Goff of the Princeton University Chemical Engineering Department; N. Seeman of the New York University Chemistry Department; and our colleagues Shyamsunder Erramilli, Jim Brody, and Fernando Camilo in the Physics Department for helpful discussions. T.D. acknowledges support from the Princeton Materials Institute. This work was supported by National Science Foundation Grant MCB-9202170, Office of Naval Research Grant N00014-91-J-4084, and National Institutes of Health Grant HG00482.

1. Volkmuth, W. D. & Austin, R. H. (1992) *Nature (London)* **358,** 600–602.
2. Smisek, D. L. & Hoagland, D. A. (1990) *Science* **248,** 1221–1223.
3. Seeman, N. C., Chen, J.-H. & Kallenbach, N. R. (1989) *Electrophoresis* **10,** 345–354.
4. Klein, J., Fletcher, D. & Fetters, L. J. (1983) *Nature (London)* **304,** 526–527.
5. Levene, S. D. & Zimm, B. H. (1987) *Proc. Natl. Acad. Sci. USA* **84,** 4054–4057.
6. de Gennes, P. G. (1971) *J. Chem. Phys.* **55,** 572–579.
7. Obukhov, S. P., Rubinstein, M. & Duke, T. (1994) *Phys. Rev. Lett.* **73,** 1263–1266.
8. de Gennes, P. G. (1975) *J. Phys. (Paris)* **36,** 1199–1203.
9. Lumpkin, O. J., Dejardin, P. & Zimm, B. H. (1985) *Biopolymers* **24,** 1573–1574.
10. Slater, G. W. & Noolandi, J. (1985) *Phys. Rev. Lett.* **55,** 572–576.
11. Manning, G. S. (1978) *Q. Rev. Biophys.* **11,** 179–246.
12. Post, C. B. (1983) *Biopolymers* **22,** 1087–1096.
13. Bustamante, C., Marko, J. F., Siggia, E. D. & Smith, S. B. (1994) *Science* **265,** 1599–1600.
14. Volkmuth, W. D., Duke, T., Wu, M.-C., Austin, R. H. & Szabo, A. (1994) *Phys. Rev. Lett.* **72,** 2117–2120.
15. Deutsch, J. M. (1988) *Science* **240,** 922–923.
16. Gardiner, C. W., ed. (1983) *Handbook of Stochastic Methods,* Springer Series in Synergetics (Springer, New York), Vol. 13.
17. Schurr, J. M. & Smith, S. B. (1990) *Biopolymers* **29,** 1161–1165.
18. Lerman, L. S. & Frisch, H. L. (1982) *Biopolymers* **21,** 995–997.
19. Southern, E. M. (1979) *Anal. Biochem.* **100,** 319–323.
20. Heller, C., Duke, T. & Viovy, J.-L. (1994) *Biopolymers* **34,** 249–259.
21. Duke, T., Viovy, J.-L. & Semenov, A. N. (1994) *Biopolymers* **34,** 239–247.
22. Viovy, J.-L., Miomandre, F., Miquel, M.-C., Caron, F. & Sor, F. (1992) *Electrophoresis* **13,** 1–6.
23. Bustamante, C., Gurrieri, S. & Smith, S. B. (1993) *Trends Biotechnol.* **11,** 23–30.
24. Fischer, S. G. & Lerman, L. S. (1980) *Proc. Natl. Acad. Sci. USA* **77,** 4420–4424.
25. Sheffield, V. C., Cox, D. R., Lerman, L. S. & Myers, R. M. (1989) *Proc. Natl. Acad. Sci. USA* **86,** 232–236.